ICLC 14 (1987) 389-402

Measuring Oxygen Permeability of Gas Permeable Hard and Hydrogel Lenses and Flat Samples in Air*

Irving Fatt, PhD, Joseph E. Rasson, PhD and John B. Melpolder, PhD

ABSTRACT

Single-chamber polarographic procedures are widely used for measuring oxygen permeability of contact lens materials. We show here that an "edge effect" due to the finite size of the polarographic cathode is a systematic source of error with these techniques. We conclude that the "edge effect", if ignored, will give measured permeabilities that are too high. We also find that the "edge effect" is not strongly dependent on permeability and therefore the ranking of contact lens materials by permeability is almost unaffected. The "edge effect" is not greatly different for measurements made on hydrogels or gas permeable hard materials.

INTRODUCTION

Single chamber polarographic procedures have been used for measuring oxygen permeability of contact lens materials since 1971. In this procedure the cathode is smaller than the lens; cathodes are from 4mm to 7mm in diameter. The collection area for oxygen at the anterior surface of the lens (the surface away from the cathode) is greater than at the cathode (see Figure 1). The combination of a cathode smaller than the lens and a large anterior oxygen collection area introduces an "edge effect" into the permeability measurement. The magnitude of this effect varies with cathode diameter, sample thickness, and, in the case of gas permeable hard lenses,

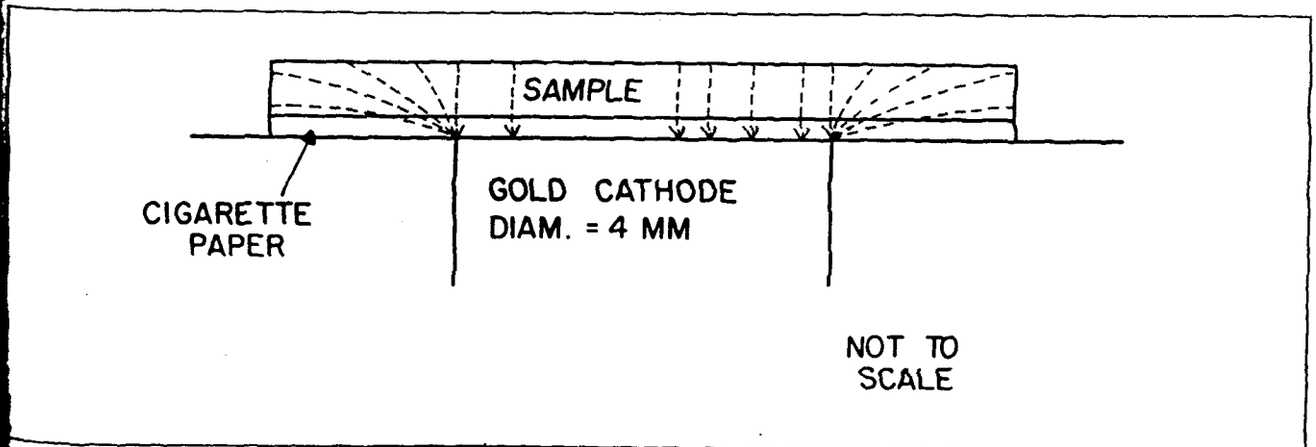

Figure 1: Schematic diagram showing a sample of gas permeable hard material on cathode of the polarographic cell. A saline-saturated layer of cigarette paper is interposed between the sample and the cathode. The diagram is not to scale.

with lens material permeability. The results of computer calculations are given here from which correction factors are obtained that compensate for the "edge effect".

THEORY OF TRANSMISSIBILITY MEASUREMENT

The basic equation for the steady-state diffusion of oxygen through a plate of area A and thickness L is Fick's Law and is stated as,

$$J = A\,(Dk/L)\,(P_2 - P_1) \qquad (1)$$

where J is the amount of oxygen that comes through in unit time, Dk is the permeability of the material, P_2 is the oxygen tension at the anterior surface of the sample, and P_1 is the oxygen tension at the surface of the sample nearest the polarographic cathode. Equation 1 requires that oxygen molecules move along parallel lines that are normal to the top and bottom surfaces of the plate of area A, as shown in Figure 1.

In the case of measurements on hydrogel materials the water needed for the cathodic reaction to occur is supplied by the hydrogel (see reference 1). However, when non-water bearing materials are measured, the water can be provided by a sheet of water-bearing substance interposed between the sample and the cathode.[2,3,4] Some investigators have used a water-based gel held on the cathode by a thin Teflon membrane, others have used saline-saturated cigarette paper.

When a water-bearing layer exists between the sample and cathode then Fick's Law, expressed as equation 1, must be modified to read,

$$J = A\,(P_2 - P_1)/(L/Dk)_w + (L/Dk)_s) \qquad (2)$$

or,

$$(A/J))\,(P_2 - P_1) = (L/Dk)_w + (L/Dk)_s \qquad (3)$$

In equation 3, the term $(A/J)\,(P_2 - P_1)$ is the reciprocal of the electrical current observed in the polarographic cell circuit at the steady state, multiplied by a constant that is the product of the number of electrons involved in the reduction of oxygen to hydroxyl ion and the Faraday. Again, it must be emphasized that equations 1, 2, and 3 apply only if the area of the cathode is the same area over which oxygen is collected at the anterior surface of the sample and the movement of oxygen is confined to a cylinder of the same cross-sectional area as the cathode.

Figure 1 shows that this condition does not hold for the arrangement of sample and cathode normally used in the single-chamber method of measuring oxygen permeability. In Figure 1 the anterior collection area is greater than the cathode area. The pattern of oxygen movement through the sample is funnel-shaped, with the narrow end of the funnel being the cathode. The area at the top of the funnel increases as sample thickness increases. The area through which oxygen moves then decreases as the oxygen approaches the cathode. The amount of oxygen entering the sample equals the amount converted to hydroxyl ions by the cathode at steady state. The resistance to movement of this oxygen is a function of the inverse of the area through which it moves. Therefore, the oxygen moving through the top of the sample encounters less resistance than the same amount of oxygen moving through the bottom of the sample. The result is that the total resistance to movement of oxygen is less than if the same amount of oxygen moved through a cylinder directly above the cathode and of the same area as the cathode. This lower resistance to oxygen movement results in higher experimentally observed polarographic electrical currents than would be observed for an ideal cylinder above the cathode. The observed electrical current is converted to an oxygen flux. Therefore there are two oxygen fluxes; one is the ideal that would be observed in the case of the ideal cylinder, the other is the observed flux in the presence of the funnel-like movement of oxygen. The flux ratio is the observed experimental flux divided by the ideal cylinder flux. The flux ratio is always greater than one when defined in this way. For the case where there is only a single kind of permeable material above the cathode, as may be true for hydrogels, the flux ratio depends only on the cathode diameter, the sample diameter, and the sample thickness. For GPH materials there are two layers, the wet cigarette paper and the GPH sample. In this case the flux ratio depends not only on the factors listed above for hydrogels but also on the permeability of the GPH sample. It can be seen that the hydrogel can be treated as a special case where the wet cigarette paper and the sample have the same permeability.

Bearing in mind that the term A in equations 1, 2, and 3 is not exactly the cathode area, we proceed to analyze equation 3 in terms of the resistance to oxygen diffusion in the water under the sample, $(L/Dk)_w$, and $(L/Dk)_s$ of the sample itself. We will add another term $(L/Dk)_{BL}$ to take into account any diffusion resistance that may exist at the sample surfaces but cannot be accounted for by the layer of water between the sample and the cathode. Equation 3 can now be written as,

$$(C/i) = (L/Dk)_T = (L/Dk)_w + (L/Dk)_{BL} + L_s\,(1/Dk)_s \qquad (4)$$

In equation 4 the term C is the so-called "cell constant", i is the observed electrical current, L_s is the sample thickness, and $(1/Dk)_s$ is the reciprocal of the material permeability. The "cell constant" may or may not include the oxygen tension difference across the sample and water layer combination. If the oxygen tension difference is included in the "cell constant" then the investigator assumes that the oxygen tension at the anterior surface is the average barometric pressure in the laboratory multiplied by 0.21 and then corrected for the relative humidity in the chamber where the polarographic cell is situated. The oxygen tension at the cathode surface is always taken as zero.[5] For greater precision the investigator may use a "cell constant" that does not include the oxygen tension difference and, instead, insert this difference at each oxygen flux measurement from knowledge of the barometric pressure and relative humidity in the measuring chamber.

A plot of C/i versus L_s yields a straight line whose slope is $(1/Dk)_s$ and whose intercept on the C/i axis is $(L/Dk)_w + (L/Dk)_{BL}$. By this procedure of data analysis the permeability is obtained independent of the water layer under the sample or the boundary layers, provided these layers remain the same for the several samples of the same material but different L_s.

Application of equation 4 to a sample in air (saturated with water vapor) is straightforward. In that case the $(L/Dk)_w$ term is simply the diffusion resistance of the water-saturated cigarette paper; the air above the sample offers no resistance to oxygen diffusion. The $(L/Dk)_{BL}$

term is more difficult to explain. There may or may not be a special resistance to the entrance of oxygen into the sample at the air surface. This resistance has been studied for silicone rubber lenses where it is important.[6,7] It is probably unimportant for most GPH materials and hydrogels. In any case, the slope of the C/i versus L_s line gives the true permeability without regard to the presence of boundary effects.

If the sample is submerged in water the $(L/Dk)_w$ term refers to the diffusion resistance of the water layer above the surface in addition to any diffusion resisting layer between the sample and the cathode. The water layer on the distal surface of the sample cannot be entirely removed no matter how vigorously the water bath is stirred. This problem, together with the problem of using a reference standard in the submerged sample method, has been discussed elsewhere[8] and will not be further elaborated upon here because we will confine our discussion to a sample surrounded by air.

EFFECT OF CATHODE DIAMETER

The polarographic cell constant that allows the observed electric current to be converted to oxygen transmissibility is a direct function of cathode area. If the distal surface of the sample collects oxygen over an area the same size as the cathode and the oxygen molecules move along parallel lines, then equation 1 is exact when A is the area of the cathode. However, as Figure 1 shows, the distal collection area is greater than the cathode area. In this case the observed oxygen flux will be greater than would be expected through a sample of area A with all oxygen flux lines confined to a right cylinder of area A. Brennan et al.[9] have pointed out that as the sample thickness approaches zero the flux lines approach the condition for flow in a right cylinder of area A. They therefore suggest that a quadratic equation be empirically fitted to the C/i versus L_s data points and that the slope of this fitted curve at zero sample thickness be taken as the reciprocal of the true permeability. There are at least two disadvantages of the Brennan et al.[9] procedure. To make a satisfactory empirical fit data points are needed for thin samples. These may be difficult to manufacture from gas permeable hard materials. Each permeability determination requires a computer-assisted curve fitting procedure.

We have chosen to solve the problem of funnel-shaped oxygen movement in the sample by decomposing the sample into small elements (the finite element method) and solving the diffusion equation in each element.[10,11,12] The numerical procedure requires a high speed digital computer.

RESULTS

The computer-assisted finite element calculation yields oxygen flux through a permeable sample when a unit oxygen tension difference exists between the polarographic cathode and the open upper surface of the sample, as shown in Figure 1. The flux under the ideal condition of oxygen movment in a right cylinder of the same area as the cathode was calculated by hand from equation 1. The ratio of these two fluxes was the result desired in this study.

The flux ratio as a function of sample thickness for flat samples of GPH materials are shown in Figure 2. The cathode diameter is fixed at 4mm but the sample diameter may be any value between 6 and 10mm. Figure 3 shows the flux ratios for lenses as obtained by applying the additional correction for convergent flow as described in Appendix I.

The curves in Figures 2 and 3 for Dk of 200×10^{-11} are probably less reliable than the lines for the lower permeabilities. An alternate procedure for obtaining flux ratios as a function of sample thickness for high permeability materials will be discussed below.

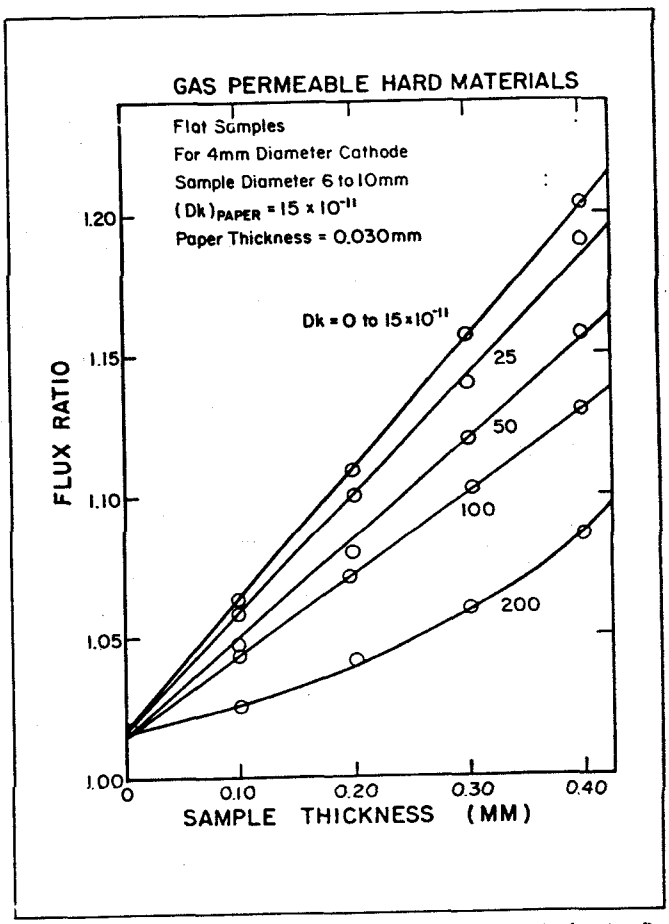

Figure 2: Ratio of oxygen flux arriving at the cathode for the flat sample compared to the flux without any edge effect. The cathode diameter is 4mm. The sample diameter may be in the range 6mm to 10mm. A layer of wet cigarette paper 0.030 mm thick and permeability 15×10^{-11} is interposed between the sample and cathode.

Figure 4 presents an experimental verification that sample diameter does not influence flux ratio when the diameter is above 6mm on a 4mm diameter cathode. A series of samples of the same GPH material, but different diameter, were measured for permeability by the procedure described in Appendix II. Samples of diameter 8, 9, and 10mm gave the same permeability corrected for edge effect. The 6mm diameter sample gave a somewhat higher permeability. All measurements were made on a

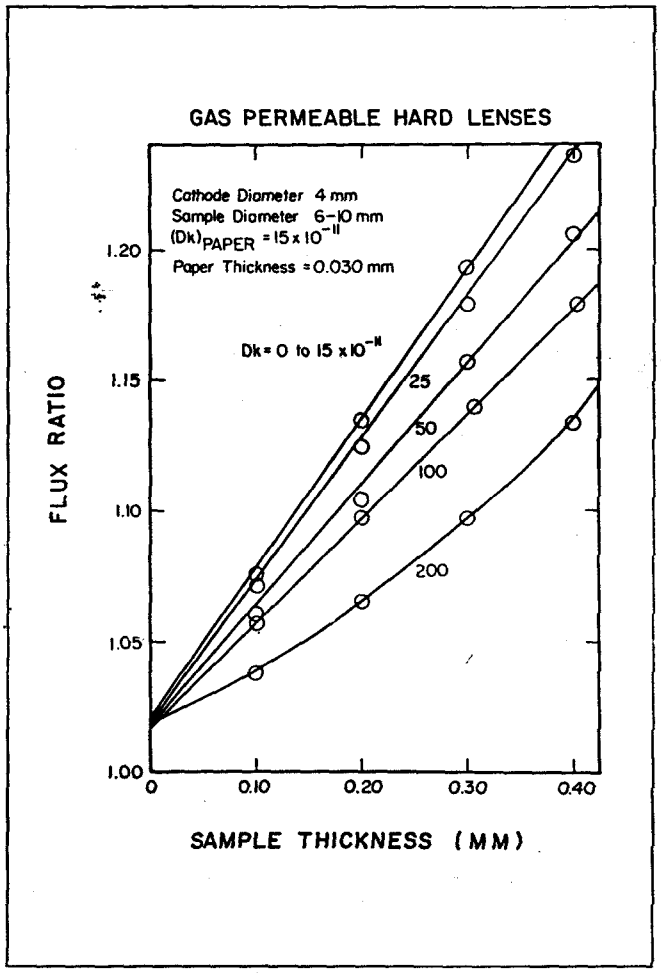

Figure 3: Same as Figure 2 except sample is in the form of a lens with parallel surfaces.

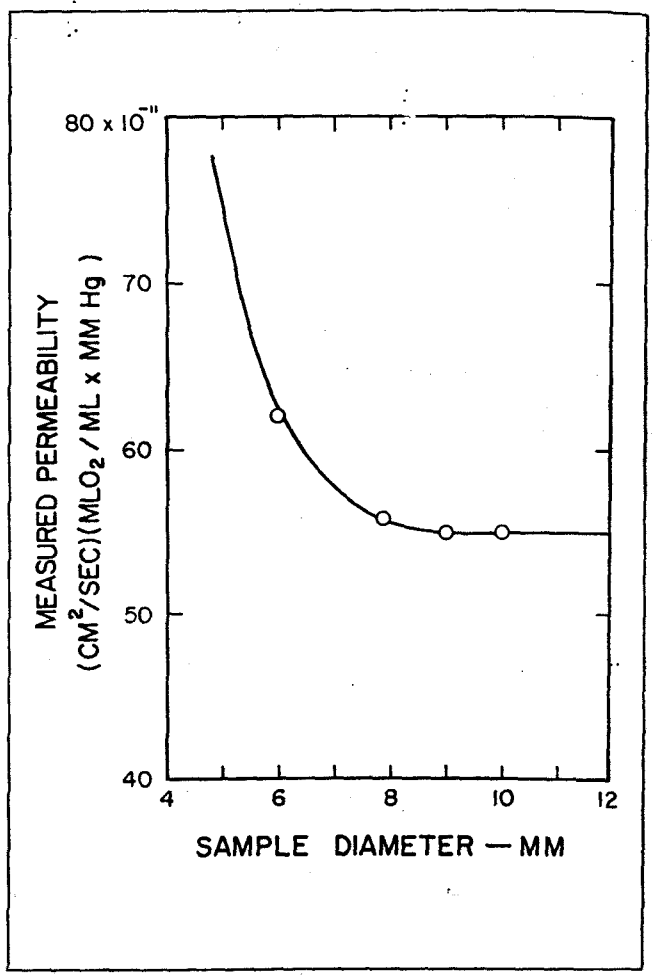

Figure 4: Measured permeability of a series of samples of the same GPH material but different diameter.

4mm diameter cathode. Although other combinations of cathode and sample diameter were not examined, the implication of these measurements is that sample diameter should be at least twice the cathode diameter.

Figure 5 shows how flux ratio at any given thickness is dependent on sample permeability for flat samples of GPH material. The horizontal lines along the right hand vertical axis are at the flux ratio level for a permeability of 15×10^{-11}. The curves at each thickness are asymptotic to these lines. This is evidence that the flux ratio dependence in this graph is a consequence of the difference in permeability between the sample and the wet cigarette paper under the sample. When there is no difference the flux ratios are independent of permeability. On this basis we can use the flux ratio at a sample permeability of 15×10^{-11} for all hydrogels. For hydrogels we can assume that there is a negligible layer between the sample and cathode, and therefore, all hydrogels, regardless of permeability, will have the flux ratio relationship shown in Figures 2 and 3 for a permeability of 15×10^{-11}. It is of interest to note that the computer calculation showed a negligible difference in flux ratio relationship between a sample permeability of 15×10^{-11} and all lower permeabilities. For this reason the lines in Figures 2 and 3 for 15×10^{-11} permeability are to be used for all lower permeabilities.

Table I gives the equations of the straight lines in Figures 2 and 3. Note that the slope of the lines for hydrogels, as shown in the last two entries in Table I, are for the lines of 15×10^{-11} permeability but the intercept terms are not the same. This is a consequence of assuming that for hydrogels there is no water layer between the sample and cathode.

The investigator who has measured $(L/Dk)_m$ on a series of samples of the same material but different thickness can easily convert the observed $(L/Dk)_m$ to the true (L/Dk) in the absence of edge effects through the use of Figures 2 and 3. Each measured $(L/Dk)_m$ point is multiplied by the flux ratio term in Figures 2 and 3 appropriate to the sample thickness and estimated or guessed permeability. A plot of these corrected (L Dk) should be linear with slope equal to the true permeability.

Appendix II shows the inverse of the method of correcting measured permeability to give true permeability. In Appendix II a series of samples of known permeability were used to calculate what the observed $(L/Dk)_m$ would have been in the presence of an edge effect. These values of $(L/Dk)_m$ were then fitted to a straight line and an erroneous permeability, $(Dk)_m$ was calculated to show the ratio of the true permeability to a permeability calculated without regard to edge effect. Figure 6 shows the error in the measured permeability as a function of the

measured permeability. In Figure 6 we see that, for example, when a measured permeability of a gas permeable hard lens is 75 × 10^{-11} this value is about 123% of the true permeability. The true permeability is then calculated to be 61 × 10^{-11}. Hydrogel lenses measured on a curved cathode are all 131% too high in measured permeability. If the hydrogel is a flat sample or the lens is pressed down on a flat cathode then the measured permeability is 124% of the true permeability for all permeabilities.

Figure 5 shows that when sample permeability is 100 × 10^{-11} or above, the flux ratio is changing rapidly with change in permeability. This effect may lead to uncertainties in the computer calculation of flux ratios for various sample thicknesses. The curved relationships in Figures 2 and 3 for material of permeability 200 × 10^{-11} may be an artifact caused by computational difficulties. A procedure that yields linear relationships between flux ratio and thickness at high permeability is described in Appendix III. When correcting permeability measurements made on silicone rubber the flux ratio equations given in Table A-III-1 should be used.

DISCUSSION

Oxygen permeability of a contact lens material as reported from laboratory measurements will be to a degree uncertain because of random and systematic errors. The random errors can be reduced by replicate measurements and quantified by statistical analysis of the data.[8] The systematic errors are more difficult to evaluate.

In the single-chamber polarographic method the per-

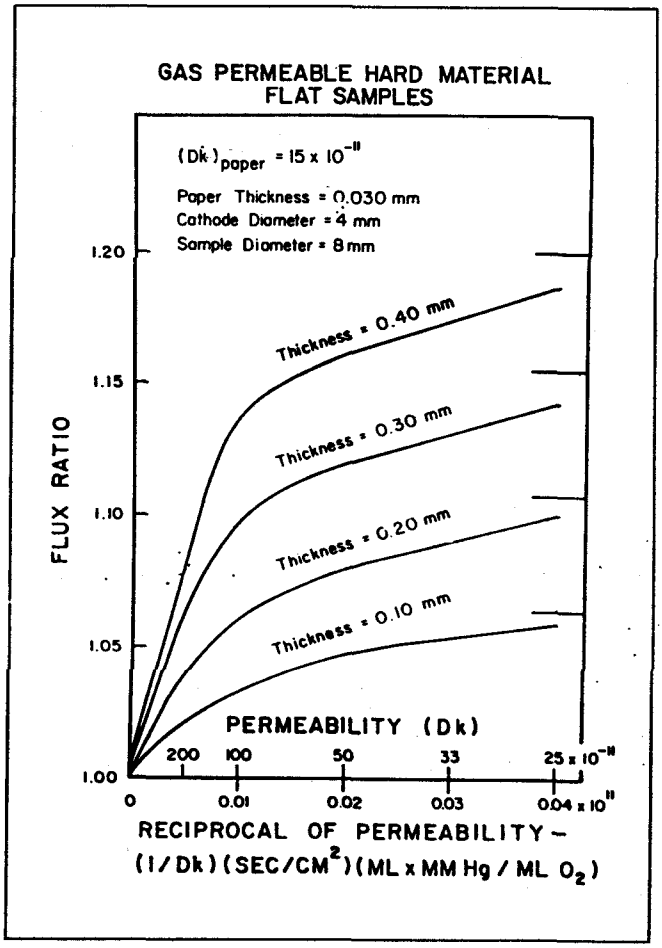

Figure 5: Calculated flux ratios as a function of reciprocal of permeability for various thicknesses. All samples were 8mm in diameter; cathode diameter was 4mm. Horizontal lines on the right hand vertical axis are the flux ratios for a permeability of 15 × 10^{-11}

TABLE I
Equations of Flux Ratio versus Thickness Lines in Figures 2 and 3
Applicable to Gas Permeable Flats and Lenses

Sample	Permeability*	Equation
Flat	0-15 × 10^{-11}	Flux Ratio = 1.017 + 4.72 L_{cm}
Flat	25	Flux Ratio = 1.017 + 4.21 L_{cm}
Flat	50	Flux Ratio = 1.015 + 3.50 L_{cm}
Flat	100	Flux Ratio = 1.014 + 2.90 L_{cm}
Flat	200	no straight line fit
Lens	0-15	Flux Ratio = 1.017 + 5.88 L_{cm}
Lens	25	Flux Ratio = 1.019 + 5.36 L_{cm}
Lens	50	Flux Ratio = 1.017 + 4.66 L_{cm}
Lens	100	Flux Ratio = 1.016 + 4.06 L_{cm}
Lens	200	no straight line fit
	Applicable to Hydrogels of All Permeabilities	
Flat		Flux Ratio = 1.00 + 4.72 L_{cm}
Lens		Flux Ratio = 1.00 + 5.88 L_{cm}

* Units of Permeability are (cm^2/sec) (ml O_2/ml × mm Hg).

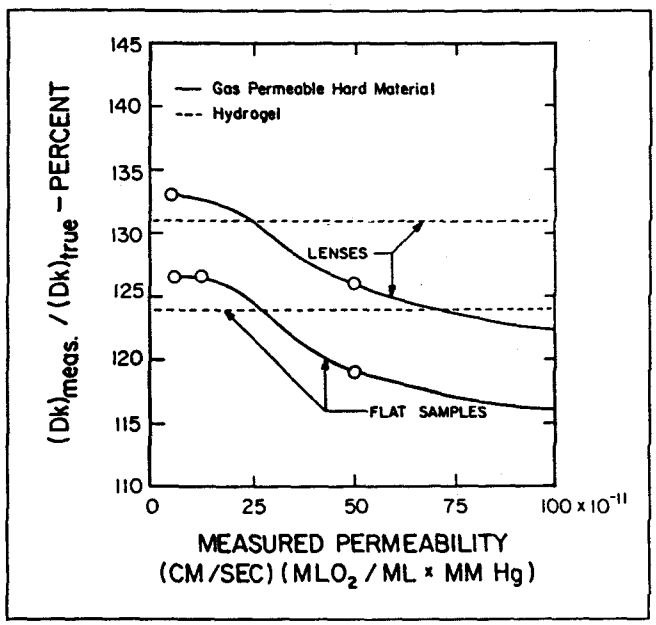

Figure 6: The ratio of measured to true permeability, as a function of measured permeability, arising from the edge effect.

meability can be reported with reference to a standard material or an absolute value can be reported if certain assumptions are made. These are: 1) The electrical equipment is accurate; 2) The number of electrons involved in the reduction of a mole of oxygen is precisely known; 3) The oxygen tension at the polarographic cathode is zero, or some other precisely known value, and it remains constant during the measurement; 4) The area of the cathode is precisely known; 5) The oxygen flux is given by equation 1, that is, the oxygen flux lines are confined to a right cylinder of the same diameter as the cathode.

If instead of an absolute value of permeability a relative value is desired, then the same standard material or materials must be available to all laboratories and all must agree on its permeability. More than one reference material may be needed because the "edge effect" is dependent on permeability.

In the absolute method the "edge effect" is a systematic error. When permeability is calculated from the polarographic current an assumption must be made concerning the geometrical relationship between the cathode area and the sample. The simplest assumption, and the one that has been used in the past, is that the movement of oxygen through the sample is confined to an area equal to that of the cathode. In reality, the path of oxygen molecules moving from the distal surface of the sample to the cathode is as shown in Figure 1. The assumption that oxygen movement is confined to a volume directly above the cathode leads to an overestimation of about 30% for low permeability hard lenses and 25% for higher permeability hard lenses. Low permeability flat samples of hard material will be about 25% too high while high permeability flat samples will be about 16% too high. For hydrogels, the measured permeability will be 30% too high for all hydrogel lenses measured on a curved cath-

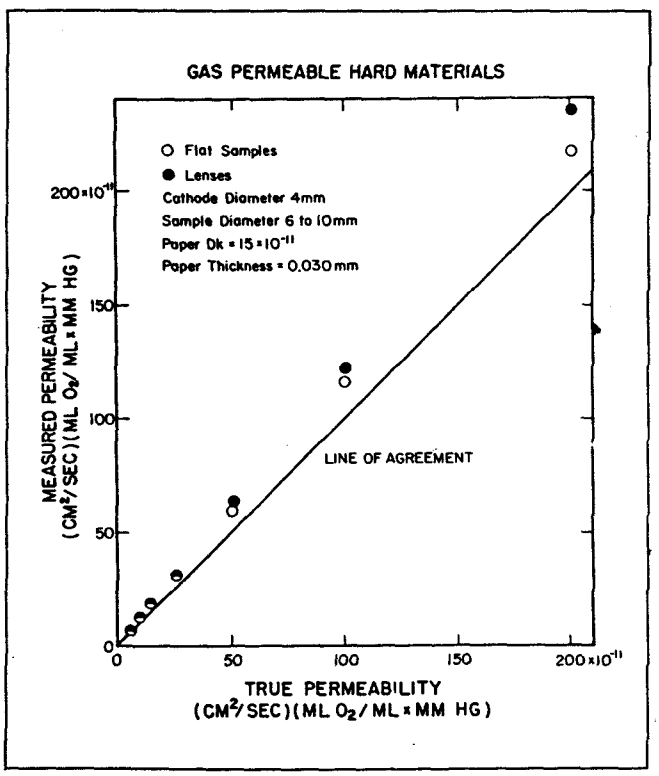

Figure 7: Measured permeability as a function of true permeability for gas permeable hard lenses and flats. If there were no edge effect, all points would lie on the line of agreement.

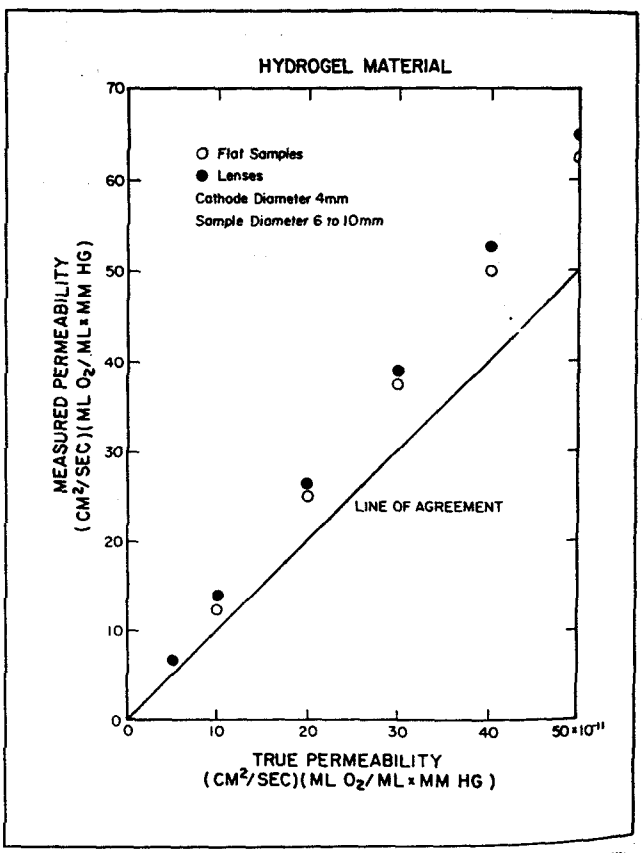

Figure 8: Measured permeability as a function of true permeability for hydrogel lenses and flats. If there were no edge effect, all points would lie on the line of agreement. Although the percentage difference between measured and true permeability of hydrogels is independent of true permeability, the absolute difference does depend on true permeability.

ode, and 24% too high when measured in the form of flats or lenses pressed onto a flat cathode. The overestimations described here are based on a cathode diameter of 4mm and a sample diameter of at least twice that amount. If the sample is less than twice the cathode diameter, then the amount of oxygen coming through the edges becomes very high. Figure 4 shows the effect on measured permeability of a small sample.

The overestimation of permeability due to the edge effect is demonstrated in Figures 7 and 8 for gas permeable hard materials and hydrogels respectively. These graphs show that the absolute difference between true and measured permeability is higher for high permeability materials, even though the percentage error is less for high permeable hard materials and independent of permeability for hydrogels.

The most extensive study of gas permeable hard lens materials has been made by the single chamber polarographic method.[8] In this study, permeabilities of 14 materials were reported. No edge effect correction was made so the permeabilities are overestimated. However, the data can be converted to a comparative study by taking one of the 14 materials as a standard and ranking all the others in relation to it. Table II shows the 14 materials with the 3M Flurofocon A material arbitrarily taken as 100. The relative permeabilities without an edge effect are shown in column 4. Column 5 shows that the materials would rank in the same order when the edge effect correction is made but the actual relative permeabilities would be slightly different.

CONCLUSIONS

1. The assumption of all oxygen movement through the sample in a direction normal to the cathode surface is invalid. An edge effect correction of 15-40% must be made to account for oxygen that enters the sample from a distal surface area that is larger than the cathode area.
2. The edge effect is different for lenses and flat samples.
3. The edge effect correction is dependent on permeability for gas permeable hard materials.
4. If one oxygen permeable material is taken as a reference, then all others can be compared to it, thereby giving a "relative permeability" that is almost independent of permeability.
5. Lenses for permeability studies should be at least twice the diameter of the cathode.

TABLE II
Permeability and Relative Permeability at 35° C of Gas Permeable Hard Materials

(1) Material	(2) Permeability* @ 35° C without edge effect correction	(3) Permeability* @ 35° C with edge effect correction	(4) Relative Permeability without edge effect correction	(5) Relative Permeability with edge effect correction
3M	95×10^{-11}	78×10^{-11}	100	100
Paraperm EW II	92	75	97	96
Optacryl Z	67	54	71	69
Alberta Supra B	66	53	69	68
Equalens	55	44	58	56
Optacryl EXT	54	43	57	55
Paraperm EW	49	39	52	50
Alberta N	40	31	42	40
Paraperm O_2 Plus	39	31	41	40
Alberta 3	36	28	38	36
Boston IV	24	18	25	23
Alberta 2	22	17	23	22
Paraperm O_2	18	14	19	18
Boston II	14	11	15	14

* Units of Permeability are (cm^2/sec) (ml O_2/ml × mm Hg).

APPENDIX I

Oxygen Transport in a Lens Compared to a Flat Disc of the Same Area

Measurement of oxygen permeability of contact lens materials can be made on lenses or flat discs. In the case of a lens there is a slight convergence of the oxygen flux lines because of the curvature. This effect gives a slightly higher oxygen transport through a lens compared to a flat sample when the polarographic cathode has the same area in both cases. Figure 9 shows the convergent flux lines for a lens.

Rationale for a Curved Surface Sensor and Measurements on Contact Lenses. In an earlier study[3] it was demonstrated that flat samples and finished lenses of the same material yielded the same permeability values within the precision of the measurements made in that study. We will show here, however, that the edge correction is greater for lenses than for flat samples. Since the edge correction introduces some uncertainty in the measured permeability there would appear to be reason to make all measurements on flat samples. This conclusion is, however, not warranted. The new high permeability hard materials are often not available as flat discs, particularly if the material is designed for molded lenses. Machining of lenses is a very different procedure from that used in preparing flat samples so if measurements of permeability are to have any clinical relevance they should be made on lenses. Finally it must be borne in mind that flat samples must be obtained from the manufacturer of the polymer. He may have an interest in the outcome of the measurement. When measurements can be made on lenses it is possible to obtain lenses anonymously from distributors or clinics.

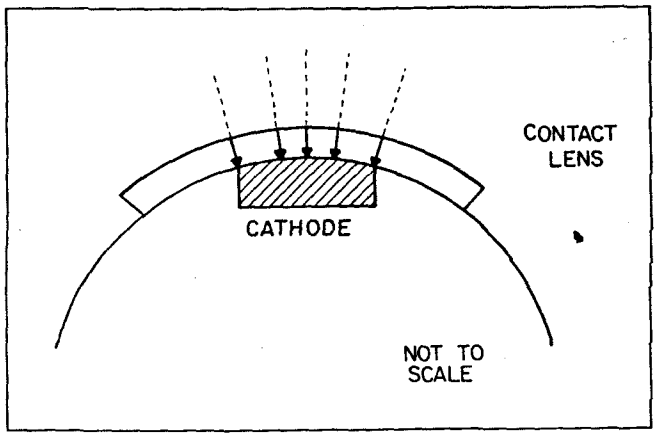

Figure 9: Schematic diagram of a lens on a cathode. The effect of the convergent oxygen flux lines due to the spherical surfaces of the lens must be added to the effects of convergence shown in Figure 1 for the flat sample.

The curved sensor does pose some problems but they can be solved. Lenses for permeability measurements must be an alignment fit on the sensor; a poor fit may lead to lens breakage. The curved sensor is best used in an air bath where the temperature is more difficult to control than in a water bath. The advantage of the air bath is that there is no need for stirring, whereas in the water bath, adequate stirring is essential. Even with vigorous stirring there is no assurance that the stagnant water layer on the sample surface can be made reproducible from one sample to another.

The comparison between a lens and a flat sample can be derived as follows.

Fick's law of steady state diffusion through a thin sphere is written,

$$J = ADk\ (dP/dr) \qquad \text{(A-I-1)}$$

where J is the oxygen transport rate, A is the area of the sphere, Dk is the permeability of the material, and dP/dr is the oxygen tension gradient across an infinitesimally thin shell. The area of a sphere is $4\pi r^2$ so equation A-I-1 becomes,

$$J = 4\pi r^2 Dk\ (dP/dr) \qquad \text{(A-I-2)}$$

Rearranging equation A-I-2 and integrating gives,

$$J = Dk\ \ dP/4\pi\ \ (dr/r^2) \qquad \text{(A-I-3)}$$

For a shell, the inside radius is taken as r_1 and outside radius as r_2. The oxygen tensions are P_1 and P_2 at these points. Integration of equation A-I-3 for a lens in the form of a hemisphere gives,

$$J_{ss} = 2\pi\ Dk\ (P_2 - P_1) / ((l/r_1) - (l/r_2)) \qquad \text{(A-I-4)}$$

where the subscript ss is added to indicate a spherical shell. This hemisphere will have an inside surface area of $2\pi r_1^2$

A flat sample of the same material on a flat polarographic cathode will allow an oxygen transport of,

$$J_F = 2\pi r_1^2\ D(P_1 - P_2) / (r_1 - r_2) \qquad \text{(A-I-5)}$$

where the subscript F indicates a flat cathode and $r_1 - r_2$ is simply the thickness of the sample.

Dividing equation A-I-4 by equation A-I-5 gives,

$$J_{ss}/J_F = r_2/r_1 \qquad \text{(A-I-6)}$$

For a lens of front radius 8.3mm and base curve 8.2mm (thickness of 0.10mm) the ratio is 1.012. The ratios for thicker lenses, all with base curve 8.2mm, are: 0.2mm, 1.024; 0.30mm, 1.037; and 0.40mm, 1.049. These oxygen transport ratios are in addition to any oxygen movement near the edge of the sample that can be attributed to an edge effect.

APPENDIX II

Application of the Edge Effect Correction by an Equation

Fick's law of diffusion yields the expression:

$$(L/Dk)_T = (L/Dk)_p + (1/Dk)_{BL} + L_{cl}\,(1/Dk)_{cl} \qquad \text{(A-II-1)}$$

for the diffusion resistance through several layers in series in the absence of edge effects. The subscripts T, p, BL, and cl refer to total, paper, boundary layer, and contact lens (or flat sample) respectively. The L term is the center thickness of a contact lens or flat sample with parallel surfaces. If the lens has optical power outside of the range −3.00D to +3.00D the center thickness may not accurately represent the average thickness of the lens. Also, since we have not examined the effect of variation of lens thickness along its diameter on the edge effect, at present it is necessary to restrict the proposed method for correcting measured permeabilities for edge effect to parallel surface samples. For this reason permeability measurements should be made on parallel surface flat plates or spherical shells or lenses of low optical power, preferably between −1.50D and +1.50D.

The term $(L/Dk)_T$ in equation A-II-1 is calculated from the polarographic electrical current via the equation:

$$(L/Dk)_T = C/i_T \qquad \text{(A-II-2)}$$

where C is the polarographic cell constant. In practice, there is an edge effect, so the true total current i_T is not observed, but instead, a measured current i_m is recorded. Dividing the cell constant C by this measured current gives a "measured" inverse of total transmissibility that includes edge effects. That is,

$$C/i_m = (L/Dk)_m \qquad \text{(A-II-3)}$$

combining equations A-II-2 and A-II-3 gives:

$$(L/Dk)_m = (L/Dk)_T\,(i_T/i_m) \qquad \text{(A-II-4)}$$

Figures 2 and 3 show that the ratio of oxygen flux through a flat sample or lens with and without edge effect is, to a good approximation, a linear function of sample thickness for materials in the permeability range of zero to 100×10^{-11}. When the relationship between flux ratio and sample thickness is linear, we can use the properties of that linear relationship to arrive at a correction factor for permeabilities measured without regard to the edge effect correction.

We must, at this time, confine ourselves to a system in which the wet paper under a gas permeable hard sample is 0.030mm thick and has a permeability of 15×10^{-11} because these were the conditions used in calculation of the data presented in Figures 2 and 3.

For the straight lines in Figures 2 and 3 we can write:

$$(L/Dk)_m = (L/Dk)_T\,(1/(a + bL)) \qquad \text{(A-II-5)}$$

where a is the intercept and b is the slope of the lines in Figures 2 and 3. The term $(L/Dk)_T$ can be taken from equation A-II-1 and inserted into equation A-II-5 to give:

$$(L/Dk)_m = ((L/Dk)_p + (L/Dk)_{BL} + L_{cl}\,(1/Dk)_{cl})\,(1/(a + bL)) \qquad \text{(A-II-6)}$$

The procedure for measuring oxygen permeability requires that $(L/Dk)_m$ is plotted as a function of L_{cl} to give a straight line of slope $(1/Dk)_{cl}$. Equation A-II-6 however will not yield a straight line if $(L/Dk)_m$ is plotted as a function of L. The data will approach a straight line only as L approaches zero or as the edge effect approaches zero. This effect is illustrated in Figure 10.

The practical implications of equation A-II-6 can be demonstrated by assuming several values of $(Dk)_{cl}$ and using observed values of $(L/Dk)_p + (L/Dk)_{BL}$ and then calculating $(L/Dk)_m$. The calculated $(L/Dk)_m$ is plotted as a function of L and a least squares line is fitted to the result.

The slope of this straight line gives a calculated $(Dk)_{cl}$ that can be compared to the true value of $(Dk)_{cl}$ that was assumed when $(L/Dk)_m$ was calculated from equation A-II-6.

Tables A-II-1 through A-II-4 give $(L/Dk)_m$ for four lenses, or flat sample thicknesses from 0.1mm to 0.4mm for both gas permeable hard materials and hydrogels. Note that the thicknesses given in the tables are in cm. The values of $(Dk/L)_m$ listed in the tables are those that would be observed in the presence of edge effects. These $(L/Dk)_m$ values are used to fit a straight line to $(L/Dk)_m$ versus L for each true value of Dk. The equation of the line is:

$$(L/Dk)_m = G + HL \qquad \text{(A-II-7)}$$

where $G = (L/Dk)_p + (L/Dk)_{BL}$ and $H = (1/Dk)_m$. To make the calculation representative of laboratory practice only $(L/Dk)_m$ from samples of thicknesses 0.10, 0.20, 0.30, and 0.40mm were used. The dotted lines in Figure 10 show that the least square lines are a good fit to the points if no thicknesses above 0.40mm are used. Figure 10 also shows the difference between (L/Dk) that would be observed in the absence of edge effects, the heavy dashed lines, and the actual $(L/Dk)_m$ observed in the presence of edge effects for the two lens samples used in this example.

Figure 10 demonstates that for samples of the thickness used in laboratory measurement of permeability there is little deviation from a straight line unless the lens is thicker than 0.30mm. Therefore linearity of measured (L/Dk) versus L cannot be taken as evidence for the absence of an edge effect. The edge effect is present in the data of Tables A-II-1 through A-II-4 and causes the calculated Dk values to be 15-35% too high. Figure 6 shows that the overestimation of Dk is greater for low permeability hard materials and for lenses compared to flat samples. For hydrogels, the overestimation is independent of permeability, but is higher for lenses than for flat samples.

For the new very high permeability hard materials, above 75×10^{-11}, the overestimation of measured permeability is lower than for hydrogels. This means that when hydrogel and gas permeable hard lenses are compared, using permeabilities uncorrected for edge effect, the hydrogel lens will appear to have a transmissibility advantage.

TABLE A-II-1
Measured Permeability as a Function of True Permeability for Gas Permeable Hard Lenses

Thickness		True Permeability						
cm		5×10^{-11}	10×10^{-11}	15×10^{-11}	25×10^{-11}	50×10^{-11}	100×10^{-11}	200×10^{-11}
0	$(L/Dk)_m^* =$	2.8×10^7	2.8×10^7	2.8×10^7	2.8×10^7	2.8×10^7	2.8×10^7	2.8×10^7
0.01		21.4	12.1	9.0	6.53	4.68	3.75	3.28
0.02		38.1	20.4	14.6	9.90	6.40	4.62	3.74
0.03		53.1	27.9	19.6	13.0	7.99	5.44	4.17
0.04		66.7	34.7	24.1	15.8	9.45	6.20	4.57
	r =	0.99900	0.99897	0.99899	0.99914	0.99933	0.99955	0.99951
	G =	7.07×10^7	4.95×10^7	4.23×10^7	3.60×10^7	3.16×10^7	2.96×10^7	2.87×10^7
	H =	15.1×10^9	7.54×10^9	5.03×10^9	3.08×10^9	1.59×10^9	0.82×10^9	0.43×10^9
	$(Dk)_m =$	6.63×10^{-11}	13.3×10^{-11}	19.9×10^{-11}	32.5×10^{-11}	62.9×10^{-11}	122×10^{-11}	233×10^{-11}
	$(Dk)_m / (Dk)_{true} =$	133%	133%	133%	130%	126%	122%	116%

*$(L/Dk)_m$ at L = 0 is an estimated point but is not used in the least square fit of $(L/Dk)_m$ and L that gives G and H in the equation $(L/Dk)_m = G + HL_{cm}$.

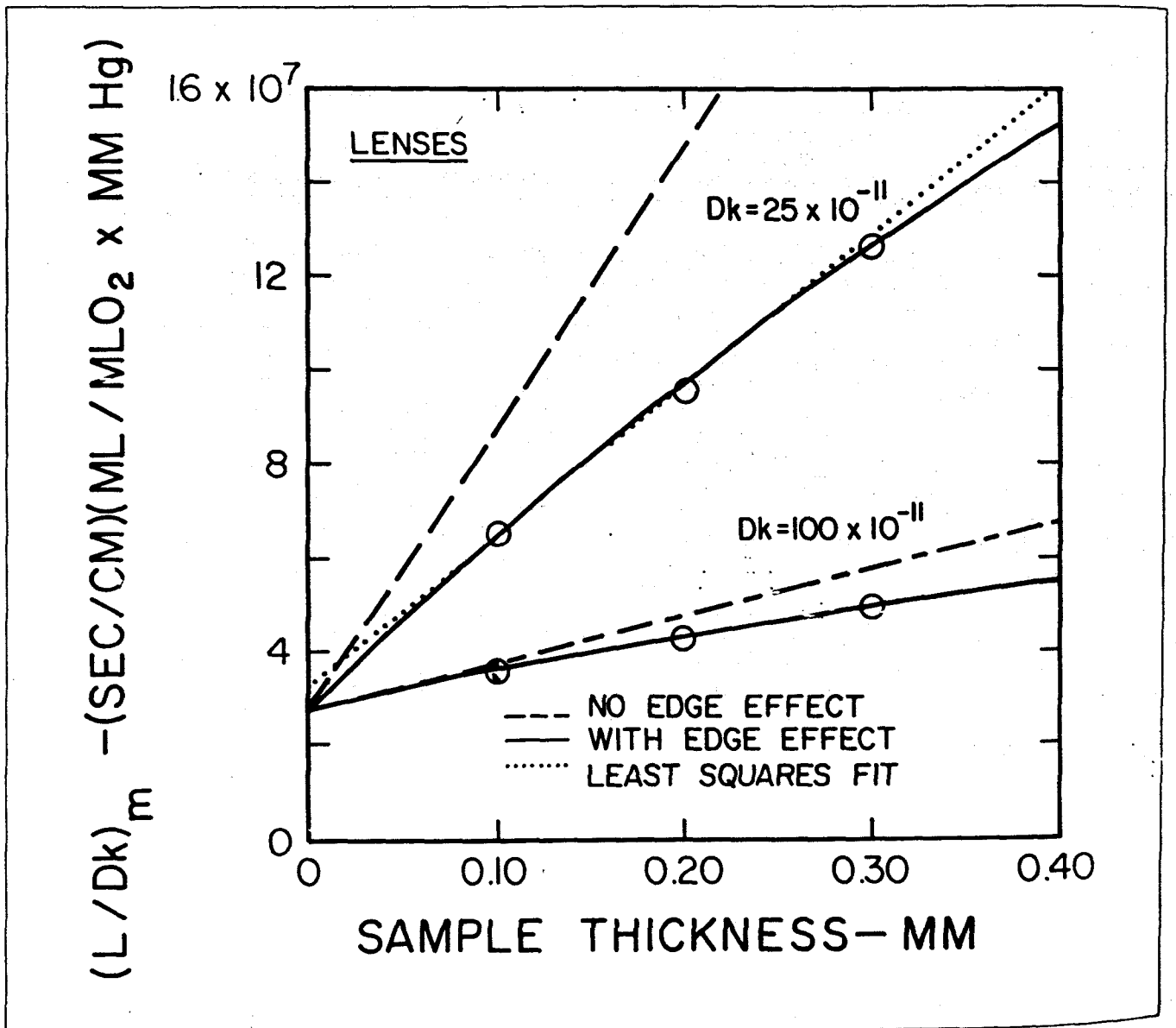

Figure 10: Sample plots of measured inverse transmissibility (polarographic cell current multiplied by cell constant) as a function of sample thickness. The solid lines are fitted through sample data points. The dashed lines are the theoretical data that would be obtained in the absence of an edge effect. The dotted lines are a line fitted by least squares through the data points that include the edge effect.

TABLE A-II-2
Measured Permeability as a Function of True Permeability for Flat Samples of Gas Permeable Hard Materials

Thickness cm		True Permeability 5×10^{-11}	10×10^{-11}	15×10^{-11}	25×10^{-11}	50×10^{-11}	100×10^{-11}	200×10^{-11}
0	$(L/Dk)_m^* =$	2.8×10^7	2.8×10^7	2.8×10^7	2.8×10^7	2.8×10^7	2.8×10^7	2.8×10^7
0.01		21.6	12.2	9.07	6.58	4.70	3.76	3.29
0.02		38.8	20.8	14.8	10.1	6.49	4.67	3.67
0.03		54.7	28.7	20.1	13.3	8.16	5.52	4.22
0.04		69.3	36.0	25.0	16.3	9.73	6.34	4.64
	r =	0.99931	0.99931	0.99931	0.99945	0.99957	0.99972	0.99769
	G =	6.41×10^7	4.61×10^7	4.00×10^7	3.46×10^7	3.08×10^7	2.93×10^7	2.81×10^7
	H =	15.9×10^9	7.93×10^9	5.29×10^9	3.24×10^9	1.68×10^9	0.86×10^9	0.46×10^9
	$(Dk)_m =$	6.30×10^{-11}	12.6×10^{-11}	18.9×10^{-11}	30.9×10^{-11}	59.7×10^{-11}	116×10^{-11}	217×10^{-11}
	$(Dk)_m / (Dk)_{true} =$	126%	126%	126%	123%	119%	116%	108%

*$(L/Dk)_m$ at L = 0 is an estimated point but is not used in the least squares fit of $(L/Dk)_m$ and L that gives G and H in the equation $(L/Dk)_m = G + HL_{cm}$.

TABLE A-II-3
Measured Permeability as a Function of True Permeability for Hydrogel Flat Samples

Thickness cm		True Permeability 5×10^{-11}	10×10^{-11}	20×10^{-11}	30×10^{-11}	40×10^{-11}	50×10^{-11}
0*	$(L/Dk)_m^* =$	0	0	0	0	0	0
0.01		19.1×10^7	9.55×10^7	4.76×10^7	3.18×10^7	2.39×10^7	1.91×10^7
0.02		36.6	18.3	9.14	6.09	4.57	3.67
0.03		52.6	26.3	13.1	8.76	6.57	5.26
0.04		67.3	33.7	16.8	11.2	8.42	6.73
	r =	0.99929	0.99929	0.99926	0.99930	0.99933	0.99918
	G =	3.71×10^7	1.86×10^7	0.92×10^7	0.62×10^7	0.47×10^7	0.38×10^7
	H =	1.61×10^{10}	8.04×10^9	4.02×10^9	2.68×10^9	2.01×10^9	1.61×10^9
	$(Dk)_m =$	6.22×10^{-11}	12.4×10^{-11}	24.9×10^{-11}	37.3×10^{-11}	49.8×10^{-11}	62.3×10^{-11}
	$(Dk)_m / (Dk)_{true} =$	124%	124%	124%	124%	124%	124%

*$(L/Dk)_m$ at L = 0 is an estimated point but is not used in the least square fit of $(L/Dk)_m$ and L that gives G and H in the equation $(L/Dk)_m = G + HL_{cm}$.

TABLE A-II-4
Measured Permeability as a Function of True Permeability for Hydrogel Lenses

Thickness cm		True Permeability 5×10^{-11}	10×10^{-11}	20×10^{-11}	30×10^{-11}	40×10^{-11}	50×10^{-11}
0*	$(L/Dk)_m^* =$	0	0	0	0	0	0
0.01		18.9×10^7	9.44×10^7	4.72×10^7	3.15×10^7	2.36×10^7	1.89×10^7
0.02		35.8	17.9	8.95	5.97	4.47	3.58
0.03		51.0	25.5	12.8	8.50	6.38	5.10
0.04		64.8	32.4	16.2	10.8	8.10	6.48
	r =	0.99895	0.99893	0.99893	0.99893	0.99895	0.99895
	G =	4.40×10^7	2.20×10^7	1.10×10^7	0.74×10^7	0.55×10^7	0.44×10^7
	H =	1.53×10^{10}	7.64×10^9	3.82×10^9	2.55×10^9	1.91×10^9	1.53×10^9
	$(Dk)_m =$	6.54×10^{-11}	13.1×10^{-11}	26.2×10^{-11}	39.3×10^{-11}	52.3×10^{-11}	65.4×10^{-11}
	$(Dk)_m / (Dk)_{true} \times$	131%	131%	131%	131%	131%	131%

*$(L/Dk)_m$ at L = 0 is an estimated point but is not used in the least square fit of $(L/Dk)_m$ and L that gives G and H in the equation $(L/Dk)_m = G + HL_{cm}$.

APPENDIX III

Flux Ratio Correction Terms for Samples of Permeability Above 100×10^{-11}

The flux ratios as functions of sample thickness, shown in Figures 2 and 3, are linear when permeability is 100×10^{-11} or less. The computer calculated flux ratios for permeability of 200×10^{-11} were not a linear function of thickness.

At this high permeability the flux ratio is a very sensitive function of permeability, as shown in Figure 5. The computational scheme may therefore have difficulty calculating the flux ratios with the necessary precision. Note that the range of flux ratios for a permeability of 200×10^{-11} is only 9% for the entire range of flat sample thicknesses from zero to 0.40mm. To circumvent this apparent computational difficulty a curve fitting scheme was used to find an equation that would linearize all of the flux ratio data of Figure 5. These equations could then be extrapolated as straight lines into the range of very high permeability materials. The linear equations that were found to give a good fit to the computed flux ratio versus permeability over the entire range of permeability from 15×10^{-11} are of the form:

$$\text{Flux Ratio} = 1.007 + a\,(L/Dk)_s/(L/Dk)_p^{\,0.268884} \qquad \text{(A-III-1)}$$

The coefficient *a* in equation A-III-1 takes on the following values for various flat sample thicknesses: 0.01cm, 0.0430; 0.02cm, 0.0650; 0.03cm, 0.0850; 0.04cm, 0.1030. For lenses, the *a* coefficients are: 0.01cm, 0.0435; 0.02cm, 0.0666; 0.03cm, 0.0881; 0.04cm, 0.1080. When the appropriate *a* term is inserted into equation A-III-1, together with estimates of reciprocal sample and paper transmissibility, the flux ratio, as a function of sample thickness, can be calculated. For sample permeabilities in the range of 15×10^{-11} to 100×10^{-11}, these flux ratios are in good agreement with flux ratios given in Figures 2 and 3. At permeability of 200×10^{-11} equation A-III-1 predicts a linear relationship between flux ratio and sample thickness rather than the curvalinear relationships shown in figures 2 and 3. The flux ratios, as linear functions of sample thickness for both flats and lenses with permeabilities of 200×10^{-11} and 400×10^{-11}, are given in Table A-III-1.

TABLE A-III-1
Equations for Flux Ratio Versus Thickness From Empirical Equations for Materials of Permeability Above 100×10^{-11}

Sample	Permeability*	Equation**
Flat	200×10^{-11}	Flux Ratio = 1.013 + 2.40 L_{cm}
Flat	400	Flux Ratio = 1.013 + 2.00 L_{cm}
Lens	200	Flux Ratio = 1.013 + 3.56 L_{cm}
Lens	400	Flux Ratio = 1.013 + 3.16 L_{cm}

*Units of Permeability are (cm^2/sec) (ml O_2/ml × mm Hg).
**These equations are for $(Dk)_p = 15 \times 10^{-11}$ and paper thickness 0.0030 cm.

*This publication is a collaborative effort of the School of Optometry, University of California, Berkeley, CA., and Bausch and Lomb, Rochester, New York.

Acknowledgement

The authors wish to thank Brien Holden for raising the issue of a boundary or edge effect and Charles Campbell for his encouragement and advice.

References

1. Fatt, I., *Polarographic Oxygen Sensors,* CRC Press, Cleveland, Ohio, page 2, 1976.
2. Refojo, M.F., Holly, F.J., and Leong, F-L. Permeability of dissolved oxygen through contact lenses. I. Cellulose acetate butyrate. *Contact Lens Intraocular Med. J.,* 3:27-33, 1977.
3. Fatt, I. Oxygen transmissibility and permeability of gas permeable hard contact lenses and materials. *ICLC,* 11:175-186, 1984.
4. Brennan, N.A., Efron, N., and Holden, B.A. Oxygen permeability of hard gas permeable contact lens materials. Clin. Exptl. Optom., 69:82-89, 1986.
5. Davies, P.W. *The Oxygen Cathode, in Physical Techniques in Biological Research, Vol. IV, Special Methods.,* L. Nastuk, Ed. Academic Press, New York, pages 137-179, 1962.
6. Hwang, S.T., Tang, T.E.S., and Kammermeyer. Transport of oxygen through silicone rubber membranes. *J. Macromol. Sci., Physics Ed.,* B5(1):1-10, 1071.
7. Fatt, I. and Chaston, J. Oxygen permeability of hydrophobic soft contact lens materials. *ICLC* 8:30-36, 1981.
8. Fatt, I., Oxygen Transmission, Chap. 10, in *Contact Lenses —The CLAO Guide to Basic Sciences and Clinical Practice, Update 2,* O.H. Dabezies, Jr., Ed., Grune & Stratton, Inc., Orlando, Florida, pages 10.1-10.48, 1987.
9. Brennan, N.A., Efron, N., and Holden, B.A. Methodology for determining the intrinsic oxygen permeability of contact lens materials. *Clin. Exptl. Optom.,* 70:42-45, 1987.
10. Tong, P., Rossettos, J.N. *Finite-Element Method—Basic Technique and Implementation,* The MIT Press, Cambridge, Mass., pages 268-274, 1977.
11. Akin, J.E. *Application and Implementation of Finite Element Methods,* Academic Press, New York, pages 245-248, 1982.
12. Dhatt, G. and Touzot, G.. *The Finite Element Method Displayed,* Wiley, New York, pages 447-480, 1984.

About the Authors

Irving Fatt, PhD, received his BS and MS degrees in chemistry from UCLA and his PhD in chemistry from USC. He was formerly senior research chemist at the Standard Oil Co. of California, where his area of study was fluid flow and diffusion in oil field rock. In 1957 he joined the engineering faculty of the Univeristy of California, Berkeley. While teaching and carrying out research on fluid flow and diffusion, Dr. Fatt also served for five years as assistant dean for graduate studies in engineering. In 1970 he became professor of physiological optics in the School of Optometry, where he has served as associate and acting dean. His work has been widely published.

John Melpolder received the BS and PhD degrees in chemistry from the University of Delaware. After a year of post-doctoral studies at the University of Delaware with Professor Heck, he joined Bausch & Lomb's Soflens Division as a senior chemist in research and development. Mr. Melpolder's current efforts include the measurement of oxygen permeability of contact lens materials and developing new polymers for contact lenses.

Joseph Rasson has the BS and MS degrees in mechanical engineering from the Chicago Campus of the University of Illinois. His PhD in mechanical engineering was obtained at the Berkeley Campus of the University of California. His PhD thesis was on the diffusion of oxygen through a multilayered system with particular application to a hydrogel contact lens on the eye. Dr. Rasson is now staff scientist at the Lawrence Berkeley Laboratory of the University of California. He is a member of the American Society of Mechanical Engineers and the American Society of Heat, Refrigeration, and Air Conditioning Engineers.